NOT TO BE CITED WITHOUT PRIOR
REFERENCE TO THE AUTHOR(S)

Northwest Atlantic Fisheries Organization

Serial No. N7514 **NAFO SCR Doc. 24/011**

SCIENTIFIC COUNCIL MEETING – JUNE 2024

Biogeochemical oceanographic conditions in the Northwest Atlantic (NAFO subareas 2-3-4) during 2023

by

D. Bélanger[1], G. Maillet[1], P. Pepin[1]

[1] Fisheries and Oceans Canada, Northwest Atlantic Fisheries Centre, P.O. Box 5667, St. John's, NL, Canada, A1C 5X1

Abstract

This report reviews the spatial and temporal variability in biogeochemical indices derived from satellite observations (spring and fall bloom timing and intensity) and in situ measurements of oceanographic variables (nitrate and chlorophyll-*a* concentration, and zooplankton abundance and biomass) across NAFO Subareas 2, 3 and 4 with an emphasis on the year 2023. Nitrate inventories on the Grand Bank and in Southern Newfoundland decreased to near-normal levels in 2023 but remained unchanged elsewhere compared to the previous year. Chlorophyll *a* inventories were variable across the zone without any strong departure from the climatological mean. Spring and fall bloom timing was later and earlier than normal, respectively, on the Scotian Shelf and the Georges Bank, while bloom intensity reached record-high levels in the Gulf of St. Lawrence in both spring and fall. Zooplankton biomass and copepod abundance were mainly near to below normal across the zone for the second consecutive year. For regions from the Grand Bank to the north, this represents a decline compared to the near to above-normal levels observed during the 2016-2021 period. The abundance of large *Calanus finmarchicus* copepods was near to above normal with no negative anomalies in any of the regions for the first time in twelve years. The abundance of smaller, but more abundant, *Pseudocalanus* spp. copepods remained high on the Grand Bank and Newfoundland Shelf, where above-normal levels have been recorded almost consistently since 2013. The abundance of non-copepod zooplankton was primarily above normal from the Grand Bank to the north, and near normal from the Scotian Shelf to the south, continuing a trend that started around the mid-2010s.

Table of Contents

Abstract 1
Table of Contents 2
1. Introduction 4
2. Methods 4
3. Results 5
  3.1. Nutrient inventories 5
  3.2. Chlorophyll *a* inventories phytoplankton bloom dynamics 5
4. Relationships between ocean climate and biogeochemical oceanographic conditions 7
5. Biogeochemical oceanographic highlights for 2023 8
Acknowledgments 8
References 9

List of Figures

Figure 1. NAFO Ecological Production Units (EPUs) used to summarize biogeochemical oceanographic conditions in the Northwest Atlantic. The Gulf of St. Lawrence is also used as a grouping unit although it is not part of NAFO EPUs. This report do not presents conditions in the Gulf of Maine and Mid-Atlantic Bight EPUs. Figure modified from Koen-Alonso et al. 2019. 12

Figure 2. (A) Location of the boxes used to calculate spring bloom indices (initiation duration, magnitude) from satellite Ocean Color imagery: (HS=Hudson Strait, NLS=northern Labrador Shelf, CLS=central Labrador Shelf, HB=Hamilton Bank, SAB=St. Anthony Basin, NENS=northeast Newfoundland Shelf, FP=Flemish Pass, FC=Flemish Cap, NGB=northern Grand Bank, SES=southeast Shoal, SPB=Green-St. Pierre Bank, NEGSL=northeast Gulf of St. Lawrence, NWGSL=northwest Gulf of St. Lawrence, MS=Magdalen Shallows, ESS=eastern Scotian Shelf, CSS=central Scotian Shelf, WSS=western Scotian Shelf. (B) Location of Atlantic Zone Monitoring Program (AZMP) oceanographic sections (black lines: BI=Beachy Island; MB=Makkovik Bank; SI=Seal Island; BB=Bonavista Bay; FC=Flemish Cap; SEGB=Southeastern Grand Bank; TBB+TCEN+TDC=Eastern Gulf of St. Lawrence; TESL+TSI+TASO=Western Gulf of St. Lawrence; TIDM=Southern Gulf of St. Lawrence; LL=Louisbourg Line; HL=Halifax Line; BBL=Brown Bank Line), and coastal high-frequency monitoring sites (red circles: S27=Station 27; R=Rimouski; S=Shediac Valley; H2=Halifax 2; P5=Prince 5) where biogeochemical data (nitrate, chlorophyll *a,* zooplankton abundance and biomass) were collected. 13

Figure 3. Top: Trends in mean annual anomalies of integrated (50-150 m) deep nitrate inventories. White open circle indicate mean annual anomalies for the Canadian Northwest Atlantic zone. Color bars indicate the relative contribution of each regions to the mean anomaly. The black line is a 3-year moving average showing the main temporal trends across the zone. Bottom: Scorecards of annual anomalies of deep nitrate inventories. White cells indicate near-normal conditions, i.e., within ± 0.5 standard deviation from the climatological mean. Blue (red) cells indicate conditions below (above) the climatological mean. Regions are listed from north to south on the left. Anomalies were calculated based on a 1999-2020 climatological period. 14

Figure 4. Top: Trends in mean annual anomalies of integrated (0-100 m) chlorophyll *a* inventories. White open circle indicate mean annual anomalies for the Canadian Northwest Atlantic zone. Color bars indicate the relative contribution of each regions to the mean anomaly. The black line is a 3-year moving average showing the main temporal trends across the zone. Bottom: Scorecards of annual anomalies of chlorophyll *a* inventories. White cells indicate near-normal conditions, i.e., within ± 0.5 standard deviation from the climatological mean. Blue (red) cells indicate conditions below (above) the climatological mean. Regions are listed from north to south on the left. Anomalies were calculated based on a 1999-2020 climatological period. 15

Figure 5. Mean timing of the (A) spring and (B) fall phytoplankton bloom within selected polygons distributed across Canadian Northwest Atlantic shelf waters (see figure 2A for polygon geographical locations). Black lines indicate the mean for the climatological period (2003-2020). Rectangles and whiskers indicate mean ±0.5, and mean ± 1 standard deviation. Polygons are listed from north to south on the left.......16
Figure 6. Scorecards of annual anomalies of spring bloom peak production timing (A), spring intensity (B), fall bloom initiation timing (C) and fall bloom intensity (D). White cells indicate near-normal conditions, i.e., within ± 0.5 standard deviation from the 2003-2020 climatological mean. Blue (red) cells indicate conditions earlier/below (later/above) the climatological mean. Regions are listed from north to south on the left. Anomalies were calculated based on a 2003-2020 climatological period. 17
Figure 7. Top: Trends in mean annual anomalies of total zooplankton biomass. White open circle indicate mean annual anomalies for the Canadian Northwest Atlantic zone. Color bars indicate the relative contribution of each regions to the mean anomaly. The black line is a 3-year moving average showing the main temporal trends across the zone. Bottom: Scorecards of annual anomalies of zooplankton biomass. White cells indicate near-normal conditions, i.e., within ± 0.5 standard deviation from the climatological mean. Blue (red) cells indicate conditions below (above) the climatological mean. Regions are listed from north to south on the left. Anomalies were calculated based on a 1999-2020 climatological period. 18
Figure 8. Top: Trends in mean annual anomalies of total copepod abundance. White open circle indicate mean annual anomalies for the Canadian Northwest Atlantic zone. Color bars indicate the relative contribution of each regions to the mean anomaly. The black line is a 3-year moving average showing the main temporal trends across the zone. Bottom: Scorecards of annual anomalies of copepod abundance. White cells indicate near-normal conditions, i.e., within ± 0.5 standard deviation from the climatological mean. Blue (red) cells indicate conditions below (above) the climatological mean. Regions are listed from north to south on the left. Anomalies were calculated based on a 1999-2020 climatological period. 19
Figure 9. Top: Trends in mean annual anomalies of non-copepod abundance. White open circle indicate mean annual anomalies for the Canadian Northwest Atlantic zone. Color bars indicate the relative contribution of each regions to the mean anomaly. The black line is a 3-year moving average showing the main temporal trends across the zone. Bottom: Scorecards of annual anomalies of non-copepod abundance. White cells indicate near-normal conditions, i.e., within ± 0.5 standard deviation from the climatological mean. Blue (red) cells indicate conditions below (above) the climatological mean. Regions are listed from north to south on the left. Anomalies were calculated based on a 1999-2020 climatological period. 20
Figure 10. Top: Trends in mean annual anomalies of *Calanus finmarchicus* abundance. White open circle indicate mean annual anomalies for the Canadian Northwest Atlantic zone. Color bars indicate the relative contribution of each regions to the mean anomaly. The black line is a 3-year moving average showing the main temporal trends across the zone. Bottom: Scorecards of annual anomalies of *Calanus finmarchicus* abundance. White cells indicate near-normal conditions, i.e., within ± 0.5 standard deviation from the climatological mean. Blue (red) cells indicate conditions below (above) the climatological mean. Regions are listed from north to south on the left. Anomalies were calculated based on a 1999-2020 climatological period. 21
Figure 11. Top: Trends in mean annual anomalies of *Pseudocalanus* spp. abundance. White open circle indicate mean annual anomalies for the Canadian Northwest Atlantic zone. Color bars indicate the relative contribution of each regions to the mean anomaly. The black line is a 3-year moving average showing the main temporal trends across the zone. Bottom: Scorecards of annual anomalies of *Pseudocalanus* spp. abundance. White cells indicate near-normal conditions, i.e., within ± 0.5 standard deviation from the climatological mean. Blue (red) cells indicate conditions below (above) the climatological mean. Regions are listed from north to south on the left. Anomalies were calculated based on a 1999-2020 climatological period. 22
Figure 12. Correlation matrix summarizing the relationships between physical (Newfoundland and Labrador climate index, winter North Atlantic Oscillation [NAO] index, air temperature, sea ice cover, sea surface temperature, and bottom temperature), and biogeochemical (phytoplankton spring bloom peak timing and intensity; integrated deep nitrate [50-150 m]; integrated chlorophyll *a* [0-100 m]; total zooplankton biomass; abundance of copepod, non-copepod, *Calanus finmarchicus*, *Pseudocalanus* spp.) indices for the Southern Newfoundland, Grand Bank, Flemish Cap, Newfoundland Shelf, and Labrador Shelf EPUs from 1999 to 2023. Green cells indicate significant positive correlation, red cells indicate significant negative correlation, and white cells indicate non-significant correlations. Numbers in cells are Pearson correlation coefficients (*r*). Significance level for Pearson correlation tests was α=0.05. 23

1. Introduction

Biogeochemical oceanographic conditions in NAFO Subareas 2, 3 and 4 are presented and interpreted in the context of long-term average conditions to provide information about broad-scale trajectories of selected indices on annual to decadal time scales. Satellite ocean colour observations and seasonal sampling of oceanographic sections and high-frequency monitoring stations by the Atlantic Zone Monitoring Program (AZMP) provided broad spatial and temporal coverage. Monitoring of standard variables (nutrients, chlorophyll *a* and zooplankton abundance and biomass) since 1999 (AZMP surveys) or 2003 (satellite ocean color observations) allows assessing spatial and temporal variability of ecologically relevant indices across the Canadian Northwest Atlantic. NAFO Ecological Production Units (EPU) and the Gulf of St. Lawrence serve as geographical grouping units to summarize biogeochemical indices at a scale deemed appropriate for integrated ecosystem management plans (Koen-Alonso et al. 2019; see Fig. 1 for EPUs location). Additional details on physical, and biogeochemical oceanographic conditions in the NWA in 2023 and earlier years can be found in Yashayaev et al. (2021), Ringuette et al. (2022), Maillet et al. (2022), Blais et al. (2023), Galbraith et al. (2023), Hebert et al. (2023), Cyr et al. (2024), Casault et al. (2024).

2. Methods

Surface chlorophyll *a* concentration was obtained from satellite observation of ocean colour by the Moderate Resolution Imaging Spectroradiometer (MODIS-Aqua) sensor (http://modis.gsfc.nasa.gov/). Daily mean surface chlorophyll *a* concentrations were used to characterize the phenology of the spring and fall phytoplankton blooms from 2003 to 2023. Estimates of the timing and intensity of the spring and fall phytoplankton blooms within polygons spanning the Canadian Northwest Atlantic (see Fig. 2A for polygon location) were obtained through the PhytoFit Shinny app (Clay et al. 2021) using a method adapted from Zhai et al. (2011).

Collection of standard AZMP variables (integrated nitrate [50-150 m] and chlorophyll *a* [0-100 m] inventories, total zooplankton biomass, and abundance of total copepods, *Calanus finmarchicus, Pseudocalanus* spp., and non-copepods) followed protocols outlined in Mitchell *et al*. (2002). Observations for 2023 and earlier years presented in this document are based on seasonal surveys conducted in spring, summer, and fall along standard AZMP oceanographic sections, and at high-frequency monitoring stations sampled at a weekly to monthly interval during the ice-free period of the year (see Fig. 2B for the location of oceanographic sections and high-frequency monitoring stations). Anomalies were used to summarize spatial and temporal variability in the biogeochemical environment at the lower trophic levels. Annual standardized anomalies were calculated for each selected variable by subtracting the mean of the reference period from the annual mean observation and by dividing the result by the standard deviation (SD) for the reference period ([observation – mean]/SD). Annual standardized anomalies for nitrate, chlorophyll, copepod, non-copepod, *Calanus finmarchicus*, and *Pseudocalanus* spp, and zooplankton biomass were calculated using the least square means of linear models that included the fixed factors Year, Season and Station (standard oceanographic sections) or Year and Month (High-frequency monitoring stations) fitted to log-transformed data (ln (x+1)). The results of this standardization yielded a series of annual anomalies that illustrate departures from the long-term average conditions, or climatology, across the range of variables. The difference between a given year and the climatological mean represents the magnitude of that departure from the reference period. The reference periods used are 2003-2020 for the spring bloom indices derived from satellite observations, and 1999-2020 for AZMP biogeochemical indices.

Anomaly values within ± 0.5 SD from the climatological mean are representative of near-normal conditions. Positive anomalies > 0.5 SD indicate conditions above (or later for bloom timing) the climatological mean. Negative anomalies < 0.5 SD indicate conditions below (or earlier for bloom timing) the climatological mean. Annual standardized anomalies of each oceanographic section and high-frequency monitoring station were averaged over NAFO EPUs and the Gulf of St. Lawrence to provide an estimate of mean oceanographic trends within each EPU. The variables selected were: spring and fall bloom timing (day of year) and intensity, i.e., mean chlorophyll *a* concentration ($mg \cdot m^{-3}$); 50-150 m integrated nitrate ($mmol \cdot m^{-2}$); 0-100 m integrated chlorophyll *a* ($mg \cdot m^{-2}$); total zooplankton biomass ($g \cdot dry\ weight \cdot m^{-2}$); and copepod, non-copepod, *Calanus* *finmarchicus*, and *Pseudocalanus* spp. abundance (ind. · m^{-2}). To estimate broad-scale spatial trends across the NWA, a weighted mean anomaly index was calculated for each sampling year by summing the annual anomalies of each AZMP oceanographic section and high-frequency monitoring station, and dividing the result by the total number of sections and stations included in the calculation.

Pearson correlation matrix quantifying the strength of the relationships between the various biogeochemical indices presented above and the physical environment was produced using the ocean climate index developed by Cyr and Galbraith (2021) for the Newfoundland and Labrador Region. We used annual anomalies of the composite climate index and of a subset of the its components, namely the winter NAO index, air temperature, sea ice extent, sea surface temperature, and bottom temperature. Biogeochemical anomalies from the Scotian Shelf and the Gulf of St. Lawrence were not included in the calculation of the correlations because these regions are not covered by the climate index.

3. Results

3.1. Nutrient inventories

Nitrate is the main limiting factor to oceanic primary production in the NWA. Nutrient concentrations in surface waters undergo seasonal fluctuations as significant nutrient uptake occurs during periods of intense phytoplankton growth during the spring and fall. Deeper inventories are less impacted by primary production processes occurring in well-lit surface waters and can be used as an index of primary production potential. General temporal patterns in integrated deep (50-150 m) nitrate inventories typically occur across a broad spatial scale in the Canadian Northwest Atlantic(Fig. 3). Nitrate inventories increased during the early 2000s and remained primarily above normal throughout the mid-2000s before declining to primarily near-to-below-normal levels over the 2010-2018 period (Fig. 3). Since 2019, nitrate inventories have remained chiefly near-to-above normal across the region (Fig. 3).

In 2023, deep nitrate inventories were above normal for a second consecutive year on the Newfoundland Shelf, reaching their highest level since the beginning of the monitoring program (Fig. 3). Nitrate inventories were near normal for a second consecutive year on the Flemish Cap but declined from record-high to near-normal levels on the Grand Bank and Southern Newfoundland (Fig. 3). The increase in nitrate inventories that occurred since 2019 was less pronounced for Gulf of St. Lawrence and the Scotian Shelf where concentrations remained primarily near-normal, with two consecutive below-normal inventories on the Scotian Shelf in 2022 and 2023 (Fig. 3). No sampling occurred on the Labrador Shelf for a second consecutive year in 2023, and although data had been collected in the Gulf of St. Lawrence, results were not available in time for this report.

3.2. Chlorophyll *a* inventories phytoplankton bloom dynamics

Chlorophyll *a* inventories were primarily near-normal throughout the 2000s, near-to-below normal during the early and mid-2010s, and near-to-above normal in the late 2010s (Fig. 4). Inventories decreased after 2020 on the Grand Bank to the north with below-normal chlorophyll *a* levels on the Newfoundland Shelf and the Labrador Shelf in 2021, and on the Grand Bank and the Flemish Cap in 2022 (Fig. 4). In 2023, chlorophyll *a* inventories were variable with below-normal levels on the Flemish Cap for a second consecutive year, above-normal levels in Southern Newfoundland and in the Gulf of St. Lawrence, and near normal levels elsewhere (Fig. 4).

Phytoplankton biomass in temperate sea undergoes seasonal variation characterized by a period of intense proliferation of large diatom cells in the spring, followed by a more modest one in the fall. In the Northwest Atlantic, the spring phytoplankton bloom coincides with the onset of water column stratification triggered by warming air temperature (Cyr et al. 2023), which occurs later at higher latitudes (Figs. 2A & 5A). Spring phytoplankton biomass typically peaks sometime between early April on the Georges Bank and Scotian Shelf, and early June off the northern Labrador Shelf (Fig. 5A). In the fall, decreasing air temperature and increased wind forcing weaken water column stratification. The replenishment of nutrient in surface waters through vertical mixing triggers the initiation of the fall bloom. Unlike the spring bloom, the timing of the fall bloom doesn't exhibit a latitudinal gradient and typically occurs between early and late September across the Northwest Atlantic, with minor regional variability (Fig. 5B).

Spring bloom timing generally exhibits substantial spatial and temporal variability, sometimes displaying broad spatial patterns such as the later-than-normal blooms of 1999 or the near-to-earlier-than-normal blooms of 2005-2006 or 2010-2011 (Fig. 6A). Despite considerable spatial variability, the peak timing of the spring bloom switched from primarily near-to-later-than-normal from 2014-2017 to primarily near-to-earlier-than-normal since around 2019, with the exception of the Georges Bank where spring bloom peak timing has remained considerably later than normal since 2020 (Fig. 6 A). Similarly to timing, spring bloom intensity does not exhibit clear broad-scale spatial or temporal patterns (Fig. 6B). However, spring bloom intensity has remained primarily near to above normal across the zone since 2021 (Fig. 6B). In 2023, the spring bloom occurred later than normal in the southernmost subregions (i.e., Georges Bank and Scotian Shelf), and mainly near normal elsewhere (Fig. 6A). Spring bloom intensity was above normal in the northernmost subregions (i.e., Newfoundland Shelf and Labrador Shelf) and in the Gulf of St. Lawrence where a time series record-high spring production was observed (Fig. 6B). Spring bloom intensity was below normal elsewhere, except for the near-normal level recorded on the Scotian Shelf (Fig. 6B).

The timing of the fall bloom is comparatively less variable than that of the spring bloom, with anomalies typically not departing strongly from the climatology (Fig. 6C). Overall, the timing of the fall bloom exhibited considerable special heterogeneity, except for 2012 and 2022 when fall bloom timing was primarily later than normal across the zone (Fig. 6C). In 2023, fall bloom timing was earlier than normal in the north (Newfound Shelf and Labrador Shelf) and especially in the south (Scotian Shel and Georges Bank), while it was slightly later than normal at mid-latitudes (Grand Bank, Flemish Cap and Southern Newfoundland) (Fig. 6C). Variation patterns in fall bloom intensity were more structured, with periods of primarily lower-than-normal intensity in 2003-2008 and 2012-2015, separated by a period of higher-than normal intensity (Fig. 6D). From 2015 through 2021, fall bloom intensity exhibited some latitudinal pattern, with generally higher intensity from the Gran Bank and Flemish Cap to the north compared to more southerly regions (Fig. 6D). This latitudinal pattern reversed in 2022 and 2023, with more intense fall blooms observed in Gulf of St. Lawrence, Scotian Shelf and Georges Bank, and less intense blooms off the Newfoundland and Labrador shelves (Fig. 6D).

3.3 Zooplankton biomass and abundance

Zooplankton are major phytoplankton consumers and, as such, are a key link between primary and secondary producers. Zooplankton biomass therefore represent an estimate of the amount of energy available to transferred to higher trophic level organisms such as fish and marine mammals. In the northwest Atlantic, both zooplankton biomass and abundance are dominated by copepods. While large copepods of the genus *Calanus* are the main drivers of total biomass, zooplankton abundance patterns are primarily driven by the abundance of small copepod taxa such as *Pseudocalanus* spp.

Zooplankton biomass peaked in the early 2000s and gradually declined across the northwest Atlantic until 2015 (Fig. 7). Biomass has since increased on the Grand Bank and Flemish Cap to the north but has remained primarily near-to-below-normal in the Gulf of St. Lawrence, on the Scotian Shelf and on the Georges Bank (Fig. 7). Temporal variation patterns in total copepod abundance generally occur at a broad spatial scale in the Northwest Atlantic. Copepod abundance gradually increased across the zone throughout the 2000s before declining slightly during the early 2010s (Fig. 8). Copepod abundance increased to near to above normal levels from 2016 through 2021 before declining again in recent years (Fig. 8). The abundance of non-copepods, mainly driven by appendicularians (pelagic tunicates) and pteropods (pelagic gastropods), markedly increased during the early 2010s and has remained high across the zone since 2016 (Fig. 9). Similarly to copepods, their abundance has been primarily above normal on the Grand Bank and Flemish Cap to the north since the mid-2010s (Fig. 9).

In 2023, zooplankton biomass were near-to-below normal across the zone for a second consecutive year (Fig. 7). This represents a decline for the Grand Bank, Flemish Cap and Newfoundland Shelf regions, but not for the Southern Newfoundland, Scotian Shelf and Gulf of St. Lawrence regions where biomass has remained near-to-below-normal for at least a decade (Fig. 7). Total copepod abundance was also near-to-below-normal across the zone for a second consecutive year in 2023 except for the Grand Bank where copepod abundance has remained primarily above normal since 2016 (Fig. 8). The decline in copepod abundance observed over the past two years mainly occurred in the Newfoundland Shelf and Flemish Cap regions (Fig. 8). As for non-copepod zooplankton, their abundance was slightly above normal on the Newfoundland Shelf and the Grand Bank and near normal elsewhere, which represented a decline from previous years and the lowest mean abundance since 2013 at the zonal scale (Fig. 9).

Calanus finmarchicus copepods are abundant and widely distributed in both coastal and offshore Northwest Atlantic waters. Although not as numerically dominant as other smaller copepod taxa, their large body size and high energy content make them major contributors to total zooplankton biomass and a high-quality food source preferentially selected by several higher trophic level species (Heat & Lough 2007; Pendleton et al. 2009, Sorochan et al. 2023). Consequently, the variability pattern of *C. finmarchicus* abundance mirrors that of total zooplankton biomass, with an increase in the early 2000s, a decline between 2010 and 2015, and another increase afterward (Fig. 10). In 2023, the abundance of *C. finmarchicus* was slightly above normal on the Scotian Shelf, the Grand Bank, and the Newfoundland Shelf, and near normal elsewhere (Fig. 10). This represented an overall increase compared to the previous year and marks the first time in 10 years without any below-normal levels across the zone (Fig. 10).

Pseudocalanus spp. are among the most abundant copepods in the Northwest Atlantic, and their seasonal and interannual abundance pattern often mirror those of other small copepod taxa (Pepin et al. 2011). Although not as energy rich as *C. finmarchicus*, *Pseudocalanus* copepods are primary food for early life stages of several ecologically and economically important species, including capelin and cod (Lynch et al. 2001; Murphy et al. 2018). The abundance pattern of *Pseudocalanus* spp. is similar to that of non-copepod zooplankton, characterized by substantially higher abundance from the mid-2010s onward compared to the 2000-2010 period (Figs. 9 & 11). In 2023, the abundance of *Pseudocalanus* spp. copepods was above normal on the Newfoundland Shelf, the Grand Bank, and in the Gul of St. Lawrence, near normal on the Flemish Cap and the Scotian Shelf, and below normal in Southern Newfoundland (Fig. 11). *Pseudocalanus* spp. abundance has been above normal since 2013 on the Grand Bank and for nine out of the past eleven years on the Newfoundland Shelf (Fig. 11). In the Gulf of St. Lawrence, above-normal abundance of *Pseudocalanus* spp. was observed for the first time since 2008 (Fig. 11).

4. Relationships between ocean climate and biogeochemical oceanographic conditions

Not surprisingly, the NL climate index is significantly correlated with most of its selected subcomponents (winter NAO, air temperature, sea ice, sea surface temperature and bottom temperature) which were also significantly intercorrelated (Fig. 12). The positive phase of the winter NAO index is associated with colder climatic conditions in the Newfoundland and Labrador region, while its negative phase is associated with warmer conditions (Colbourne et al. 1994). This aligns with the positive and negative relationships of the winter NAO with sea ice and air temperature, respectively (Fig. 12). Significant correlations between air temperature and sea ice, sea surface temperature and bottom temperature highlight the importance of atmospheric forcing on ocean climate (Fig. 12).

Significant correlations between spring bloom timing and air temperature, sea ice, and sea surface temperature indicates that warmer conditions are favourable to earlier bloom onsets (Fig. 12). Reduced sea ice cover increases access to sunlight and accelerates water column stratification through energy transfer form the warmer atmosphere to colder ocean surface (Chiswell 2011, Rumyantseva et al. 2019, Cyr et al. 2022). Additionally, freshwater input from melting sea ice further promotes early surface stratification and spring bloom onset during warmer years (Kishi et al. 2021). Chlorophyll *a* inventories measured in situ during seasonal AZMP surveys were positively correlated with deep nitrate inventories lagged by one year (Fig. 12). Nitrate is the main limiting nutrient for phytoplankton growth in temperate seas (*Howarth* 1988, Bristow et al. 2017). Nitrate concentrations in surface waters, where most of the primary production occurs, may exhibit considerable fluctuations due nutrient uptake during period of intense phytoplankton growth such as the spring and fall blooms. In contrast, nutrient inventories from deeper water are much less affected by near-surface primary production processes. Deep nutrients, therefore, represent an indicator of primary production potential for the following year after winter vertical mixing has brought them up to the surface where they can fuel phytoplankton growth.

Zooplankton biomass was positively correlated with the abundance of copepods, which in turn was correlated with the abundance of *C. finmarchicus* and *Pseudocalanus* spp. (Fig. 12). However, only the less abundant *C. finmarchicus* was correlated with total zooplankton biomass (Fig. 12), highlighting the critical role of this species in Northwest Atlantic food webs (Planque & Batten 2000 Head et al. 2003). *C. finmarchicus* are primarily herbivores with an annual life cycle. Subadults of emerge from dormancy in late winter and migrate toward the surface to moult and mate (Head et al. 2013). Females release their eggs into near-surface waters where they hatch and develop until early fall, when they return to depth to overwinter (Head & Pepin 2008, Melle et al. 2014, Head et al. 2013). Egg production in *C. finmarchicus* females is positively related to phytoplankton biomass in the North Atlantic (Jónasdóttir et al. 2002), and significant correlations *between C. finmarchicus* abundance and the NL climate index (positive correlation) and spring bloom timing (negative correlation) also suggest that early spring blooms, associated with warmer environmental conditions, favor recruitment (Cyr et al. 2023). The negative correlations between the abundance of both *Pseudocalanus* spp. and total copepods, and chlorophyll *a inventories* (Fig. 12) likely reflect the potential impact of increased grazing pressure by copepods on phytoplankton standing stock (Bautista & Harris 1992).

5. Biogeochemical oceanographic highlights for 2023

- Phytoplankton bloom intensity was at record-high level in the Gulf of St. Lawrence (spring and fall) and on the Scotian Shelf (fall).
- The abundance of large *Calanus finmarchicus* copepods was near to above normal with no negative anomalies in any of the regions for the first time in twelve years.
- The abundance of small *Pseudocalanus* spp. copepods has remained above normal for eleven consecutive years on the Grand Bank, and for nine of the past eleven years on the Newfoundland Shelf.
- The abundance of non-copepod zooplankton has declined to near normal in more than half of the regions for the first time since 2015. However, non-copepod abundance was above normal for eleven out of the past twelve years on the Grand Bank, and for seven out of the past 8 years on the Newfoundland Shelf.

Acknowledgments

We thank the personnel at the Northwest Atlantic Fisheries Center (NL Region), the Bedford Institute of Oceanography and (Maritimes Region), the Maurice -Lamontagne Institute (Quebec Region), the St. Andrews Biological Station and various offices in the Gulf Region who contributed to sample collection as well as laboratory and data analyses. We also thank the officers and crews of the Canadian Coast Guard Ships and other research vessels who assisted with the collection of oceanographic data during 2023.

References

Bautista B and Harris RP (1992) Copepod gut contents, ingestion rates and grazing impact on phytoplankton in relation to size structure of zooplankton and phytoplankton during a spring bloom. *Mar Ecol Prog Ser* 82: 41-50.

Blais M, Galbraith PS, Plourde S, Plourde S, Lehoux C (2023) Chemical and biological oceanographic conditions in the Estuary and Gulf of St. Lawrence during 2022. DFO Can. Tech. Rep. Hydrogr. Ocean Sci. 357: v + 70 p.

Bristow LA, Mohr W, Ahmerkamp S and Kuypers MM (2017) Nutrients that limit growth in the ocean. Curr *Biol* 27: R431-R510.

Casault B, Beazley L, Johnson C, Devred E and Head E (2024). Chemical and biological oceanographic conditions on the Scotian Shelf and in the eastern Gulf of Maine in 2022. DFO Can. Tech. Rep. Fish. Aquat. Sci. 3589: vi + 72 p.

Chiswell SM (2011) Annual cycles and spring blooms in phytoplankton: don't abandon Sverdrup completely. *Mar Ecol Prog Ser* 443:39-50.

Clay S, Layton C and Devred E (2021) BIO-RSG/PhytoFit: First release (v1.0.0). *Zenodo*. https://doi.org/10.5281/zenodo.4770754.

Colbourne E, Narayanan S and Prinsenberg S (1994) Climatic changes and environmental conditions in the Northwest Atlantic, 1970-1993. *ICES J of Mar Sci Symp* 198: 311-322.

Cyr F and Galbraith PS (2021) A climate index for the Newfoundland and Labrador Shelf. *Earth Syst Sci Data* 13: 1807-1828.

Cyr F, Lewis K, Bélanger D, Regular P, Clay S, Devred E (2023) Physical controls and ecological implications of the timing of the spring phytoplankton bloom on the Newfoundland and Labrador shelf. *Limnology and Oceanogr Lett* 9: 191-198.

Cyr F, Coyne J, Snook S, Bishop C, Bishop C, Galbraith PS, Chen N and Han G (2024) Physical oceanographic conditions on the Newfoundland and Labrador Shelf during 2022. Can. Tech. Rep. Hydrogr. Ocean Sci. 377: iv + 53 p.

Galbraith PS, Chassé J, Dumas J, Shaw J-L, Dumas J, Lefaivre D and Bourassa M (2023) Physical oceanographic conditions in the Gulf of St. Lawrence during 2022. Can. Tech. Rep. Hydrogr. Ocean Sci. 354: v + 88 p.

Head EJH, Harris LR and Yashayaev I (2003) Distributions of *Calanus* spp. and other mesozooplankton in the Labrador Sea in relation to hydrography in spring and summer (1995-2000). *Prog Oceanogr* 59: 1–30.

Head EJH and Pepin P (2008) Variations in overwintering depth distributions of *Calanus finmarchicus* in the slope waters of the NW Atlantic continental shelf and the Labrador Sea. *J Northwest Atl Fish* Sci 39: 49-69.

Head EHJ, Melle W, Pepin P, Bagøien E and Broms C (2013) On the ecology of *Calanus finmarchicus* in the Subarctic North Atlantic: A comparison of population dynamics and environmental conditions in areas of the Labrador Sea-Labrador/Newfoundland Shelf and Norwegian Sea Atlantic and Coastal Waters. *Prog Oceanogr* 114, 46-63.

Heath MR and Lough RG (2007) A synthesis of large-scale patterns in the planktonic prey of larval and juvenile cod (*Gadus Morhua*). *Fish Oceanogr* 16: 169-185.

Hebert D, Layton C, Brickman D and Galbraith PS (2023) Physical oceanographic conditions on the Scotian Shelf and in the Gulf of Maine during 2022. DFO Can. Tech. Rep. Hydrogr. Ocean Sci. 359: vi + 81 p.

Howart RW (2017) Nutrient limitation of net primary production in marine ecosystems. *Annual Review of Ecology and Systematics* 19: 89-110.

Jónasdóttir SH, Gudfinnsson HG, Gislason A, Astthorsson OS (2002) Diet composition and quality for *Calanus finmarchicus* egg production and hatching success off south-west Iceland. *Mar Biol* 140: 1195-1206.

Kishi S, Ohshima KI, Nishioka J, Isshiki N, Nihashi S and Riser SC (202) The prominent spring bloom and its relation to sea-ice melt in the Sea of Okhotsk, revealed by profiling floats. *Geophys Res Lett* 48: e2020GL091394.

Koen-Alonso M, Pepin P, Fogarty M, Kenny A and Kenchington E (2019) The Northwest Atlantic Fisheries Organization Roadmap for the development and implementation of an Ecosystem Approach to Fisheries: structure, state of development, and challenges. *Mar Policy* 100: 342-352.

Lynch DR, Lewis CVW, Verner FE (2001) Can Georges Bank larval cod survive on a calanoid diet? *Deep-Sea Researh II* 48: 609-630.

Maillet G, Bélanger D, Doyle G, Robar A, Rastin S, Ramsay D and Pepin P (2022) Optical, chemical and biological oceanographic conditions on the Newfoundland and Labrador Shelf during 2018. DFO Can. Sci. Advis. Sec. Res. Doc. 2022/075. Viii + 53 p.

Melle W, Runge F, Head E, Plourde S, and others (2014) The North Atlantic Ocean as habitat for *Calanus finmarchicus*: Environmental factors and life history traits. *Prog Oceanogr* 129: 244-284.

Mitchell MR, Harrison G, Pauley K, Gagné A, Maillet G and Strain P (2002) Atlantic Zone Monitoring Program Sampling Protocol. Canadian Technical Report of Hydrography and Ocean Sciences 223, 23 pp.

Murphy HM, Pepin P, and Robert D (2018) Re-visiting the drivers of capelin recruitment in Newfoundland since 1991. *Fish Res* 200: 1-10.

Pendleton DE, Pershing AJ, Brown MW, Mayo CA, Kenedy, RD, Record NR, Cole TVN (2009) Regional-scale mean copepod concentration indicates relative abundance of North Atlantic right whales. *Mar Ecol Prog Ser* 378: 211-225.

Pepin P, Colbourne E, Maillet G (2011) Seasonal patterns in zooplankton community structure on the Newfoundland and Labrador Shelf. *Prog Oceanogr* 91: 273-285

Planque B and Batten DS (2000) *Calanus finmarchicus* in the North Atlantic: the year of *Calanus* in the context of interdecadal change. *ICES J Mar Sci* 57: 1528-1535.

Plourde S, Lehoux C, Johnson CL and Lesage V (2019) North Atlantic right whale (*Eubalaena glacialis*) and its food: (I) a spatial climatology of *Calanus* biomass and potential foraging habitats in Canadian waters. *J Plankton Res* 41: 667-685.

Ringuette M, Devred E, Azetsu-Scott K, Head E, Punshon S, Casault B and Clay S (2022). Optical, chemical, and biological oceanographic conditions in the Labrador Sea between 2014 and 2018. DFO Can Sci Advis Sec Res Doc 2022/021. V + 38 p.

Rumyantseva A, Henson S, Martin A, Thompson AF, Damerell GM, Kaiser J, Heywood KJ (2019) Phytoplankton spring bloom initiation: The impact of atmospheric forcing and light in the temperate North Atlantic Ocean. *Prog Oceanogr* 178: 102202.

Sorochan KA, Plourde S and Johnson CL (2023) Near-Bottom aggregations of *Calanus* spp. copepods in the southern Gulf of St. Lawrence in summer: significance for North Atlantic right whale foraging. *ICES J Mar Sci* 80: 787-802

Yashayaev I, Peterson I and Wang Z (2021). Meteorolical, sea ice, and physical oceanographic conditions in the Labrador Sea during 2019. DFO Can. Sci. Advis. Sec. Res. Doc. 2021/074. iv +38 p.

Zhai L, Platt T, Tang C, Sathyendranath S, Walls, RH (2011) Phytoplankton phenology on the Scotian Shelf. *ICES J Mar Sci* 68: 781-791.

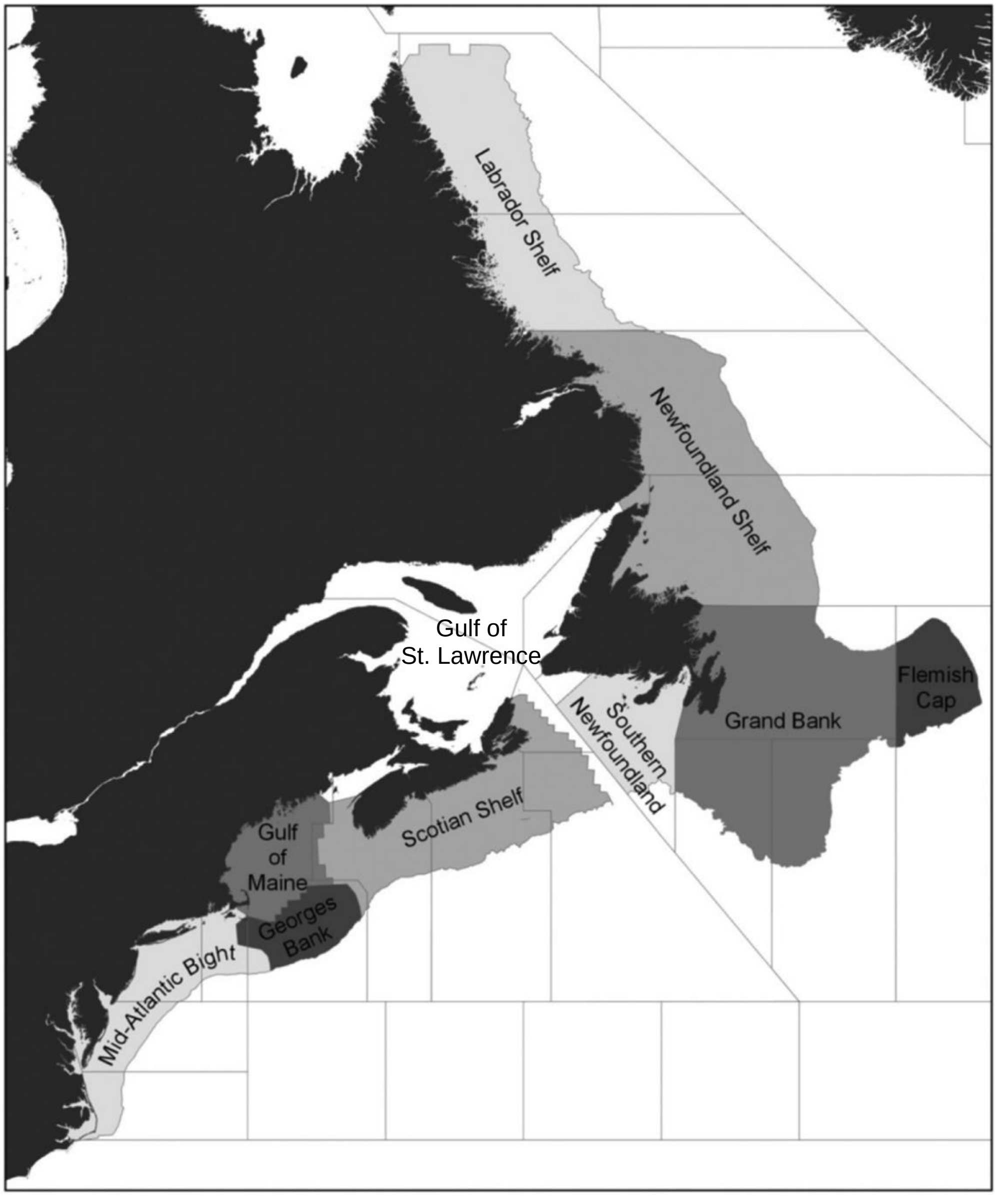

Figure 1. NAFO Ecological Production Units (EPUs) used to summarize biogeochemical oceanographic conditions in the Northwest Atlantic. The Gulf of St. Lawrence is also used as a grouping unit although it is not part of NAFO EPUs. This report do not presents conditions in the Gulf of Maine and Mid-Atlantic Bight EPUs. Figure modified from Koen-Alonso et al. 2019.

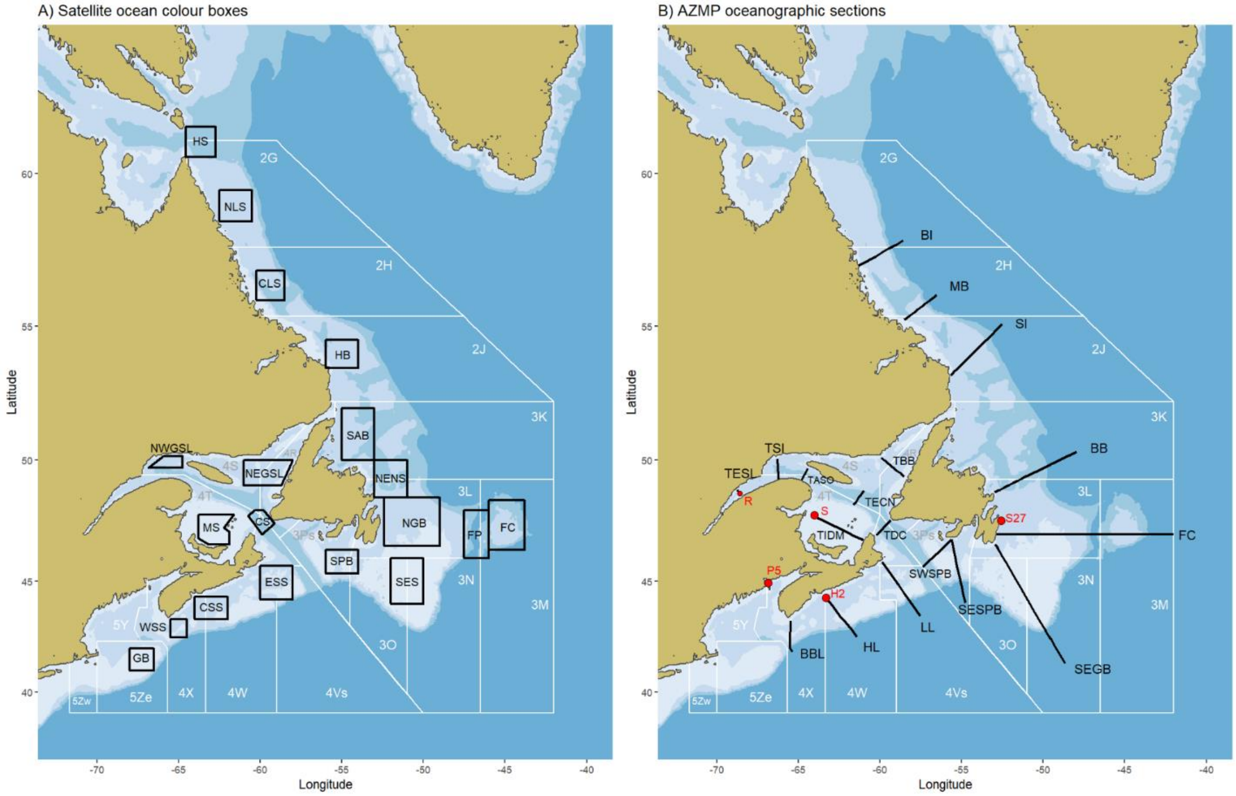

Figure 2. (A) Location of the boxes used to calculate spring bloom indices (initiation duration, magnitude) from satellite Ocean Color imagery: (HS=Hudson Strait, NLS=northern Labrador Shelf, CLS=central Labrador Shelf, HB=Hamilton Bank, SAB=St. Anthony Basin, NENS=northeast Newfoundland Shelf, FP=Flemish Pass, FC=Flemish Cap, NGB=northern Grand Bank, SES=southeast Shoal, SPB=Green-St. Pierre Bank, NEGSL=northeast Gulf of St. Lawrence, NWGSL=northwest Gulf of St. Lawrence, MS=Magdalen Shallows, ESS=eastern Scotian Shelf, CSS=central Scotian Shelf, WSS=western Scotian Shelf. (B) Location of Atlantic Zone Monitoring Program (AZMP) oceanographic sections (black lines: BI=Beachy Island; MB=Makkovik Bank; SI=Seal Island; BB=Bonavista Bay; FC=Flemish Cap; SEGB=Southeastern Grand Bank; TBB+TCEN+TDC=Eastern Gulf of St. Lawrence; TESL+TSI+TASO=Western Gulf of St. Lawrence; TIDM=Southern Gulf of St. Lawrence; LL=Louisbourg Line; HL=Halifax Line; BBL=Brown Bank Line), and coastal high-frequency monitoring sites (red circles: S27=Station 27; R=Rimouski; S=Shediac Valley; H2=Halifax 2; P5=Prince 5) where biogeochemical data (nitrate, chlorophyll *a,* zooplankton abundance and biomass) were collected.

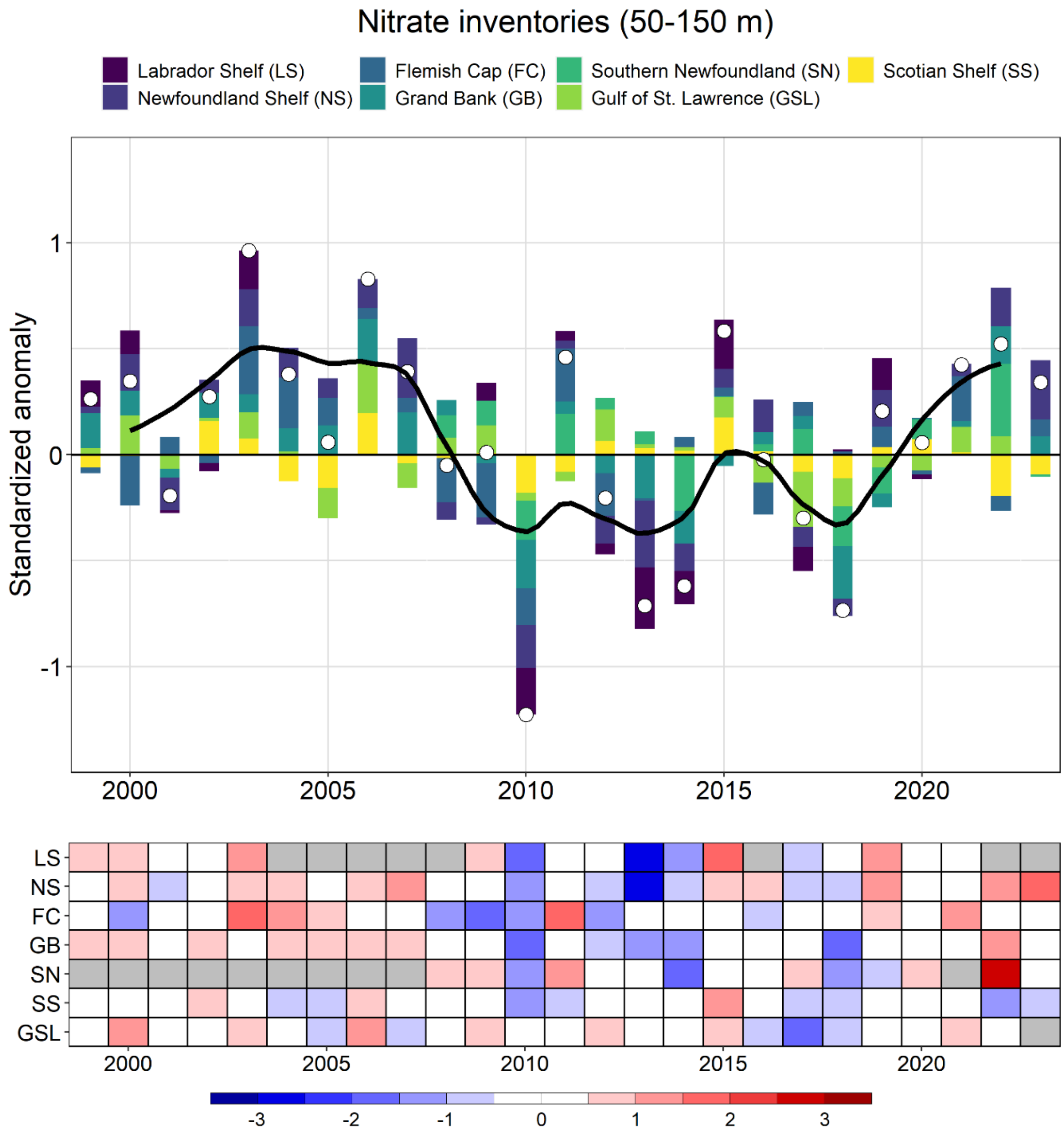

Figure 3. Top: Trends in mean annual anomalies of integrated (50-150 m) deep nitrate inventories. White open circle indicate mean annual anomalies for the Canadian Northwest Atlantic zone. Color bars indicate the relative contribution of each regions to the mean anomaly. The black line is a 3-year moving average showing the main temporal trends across the zone. Bottom: Scorecards of annual anomalies of deep nitrate inventories. White cells indicate near-normal conditions, i.e., within ± 0.5 standard deviation from the climatological mean. Blue (red) cells indicate conditions below (above) the climatological mean. Regions are listed from north to south on the left. Anomalies were calculated based on a 1999-2020 climatological period.

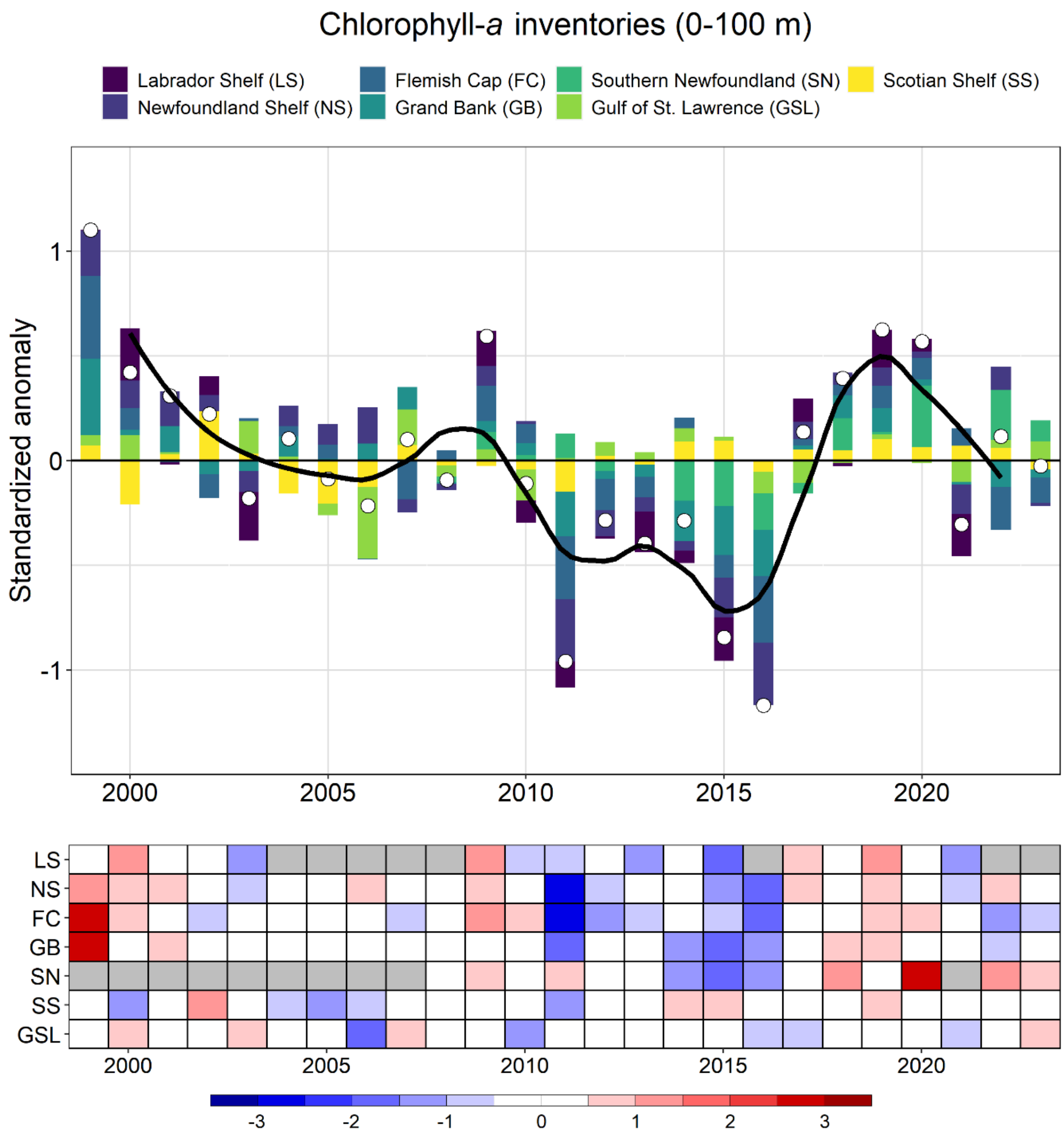

Figure 4. Top: Trends in mean annual anomalies of integrated (0-100 m) chlorophyll *a* inventories. White open circle indicate mean annual anomalies for the Canadian Northwest Atlantic zone. Color bars indicate the relative contribution of each regions to the mean anomaly. The black line is a 3-year moving average showing the main temporal trends across the zone. Bottom: Scorecards of annual anomalies of chlorophyll *a* inventories. White cells indicate near-normal conditions, i.e., within ± 0.5 standard deviation from the climatological mean. Blue (red) cells indicate conditions below (above) the climatological mean. Regions are listed from north to south on the left. Anomalies were calculated based on a 1999-2020 climatological period.

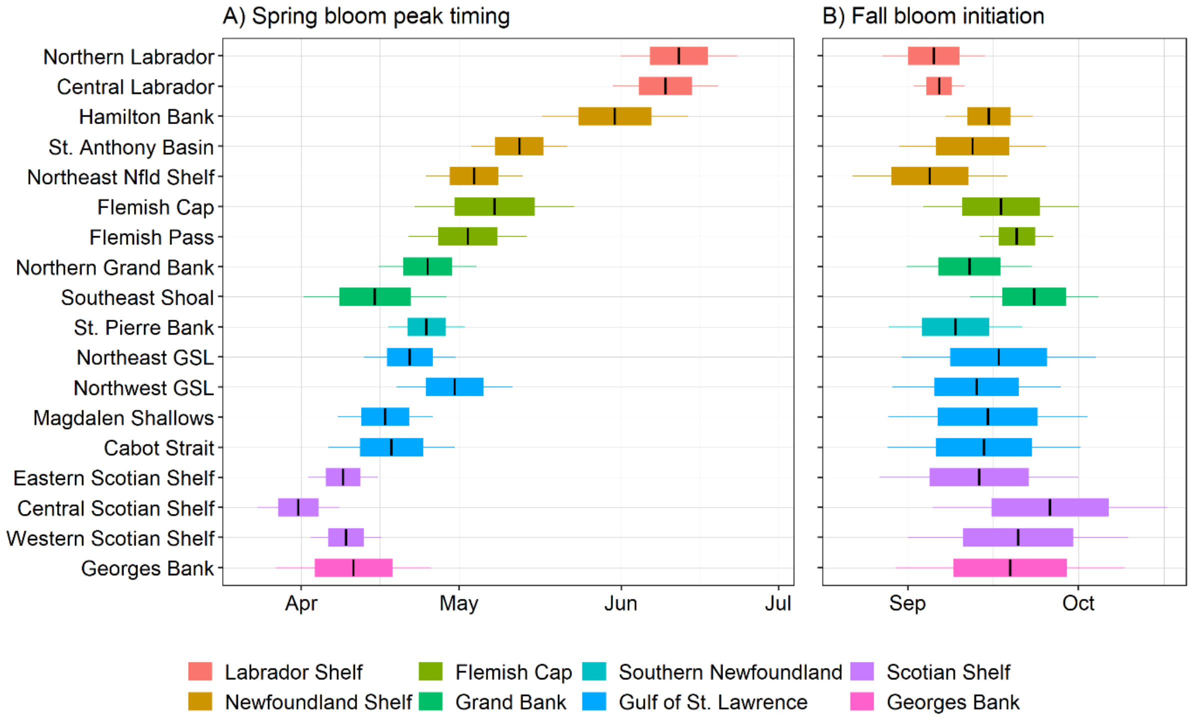

Figure 5. Mean timing of the (A) spring and (B) fall phytoplankton bloom within selected polygons distributed across Canadian Northwest Atlantic shelf waters (see figure 2A for polygon geographical locations). Black lines indicate the mean for the climatological period (2003-2020). Rectangles and whiskers indicate mean ±0.5, and mean ± 1 standard deviation. Polygons are listed from north to south on the left.

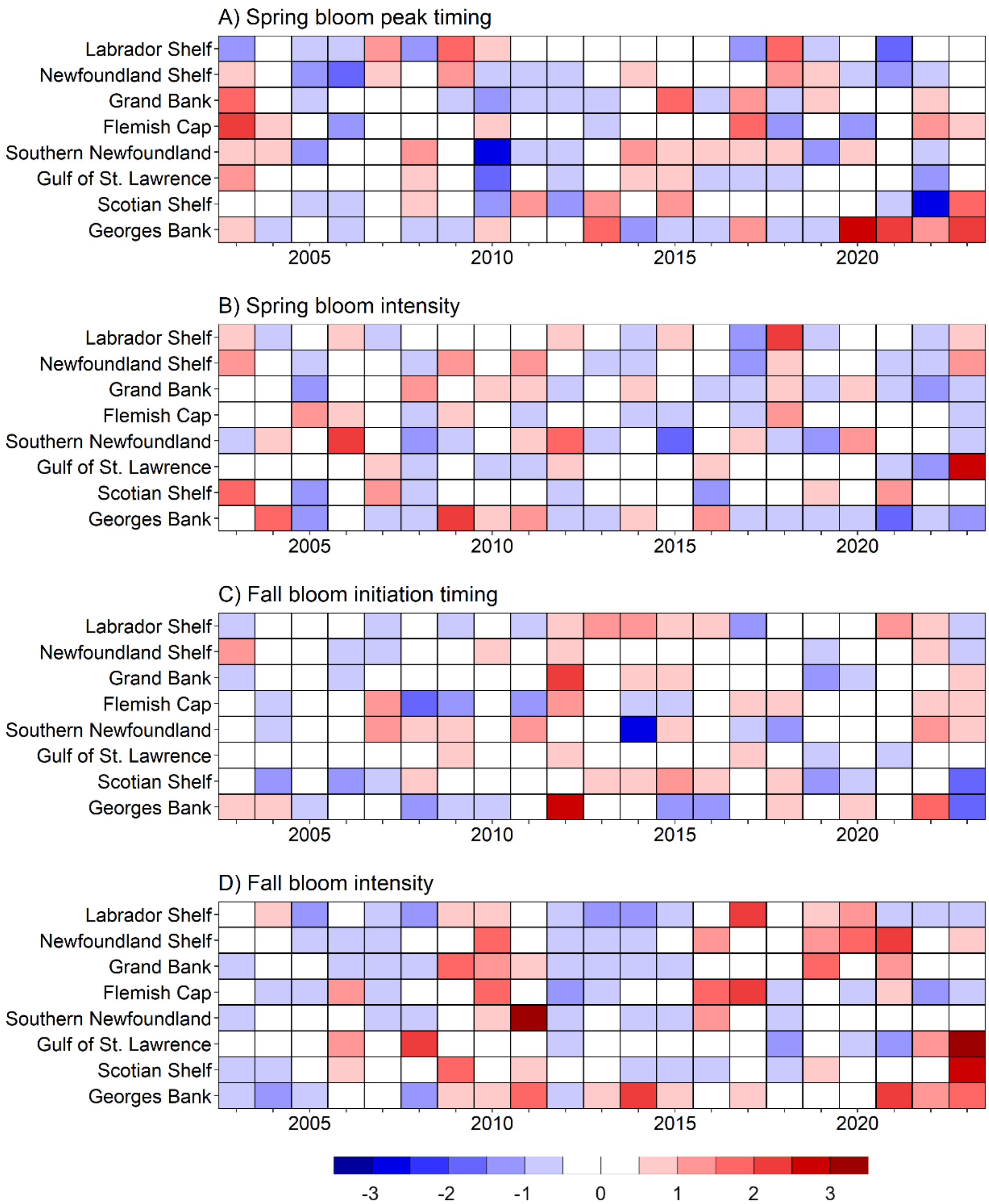

Figure 6. Scorecards of annual anomalies of spring bloom peak production timing (A), spring intensity (B), fall bloom initiation timing (C) and fall bloom intensity (D). White cells indicate near-normal conditions, i.e., within ± 0.5 standard deviation from the 2003-2020 climatological mean. Blue (red) cells indicate conditions earlier/below (later/above) the climatological mean. Regions are listed from north to south on the left. Anomalies were calculated based on a 2003-2020 climatological period.

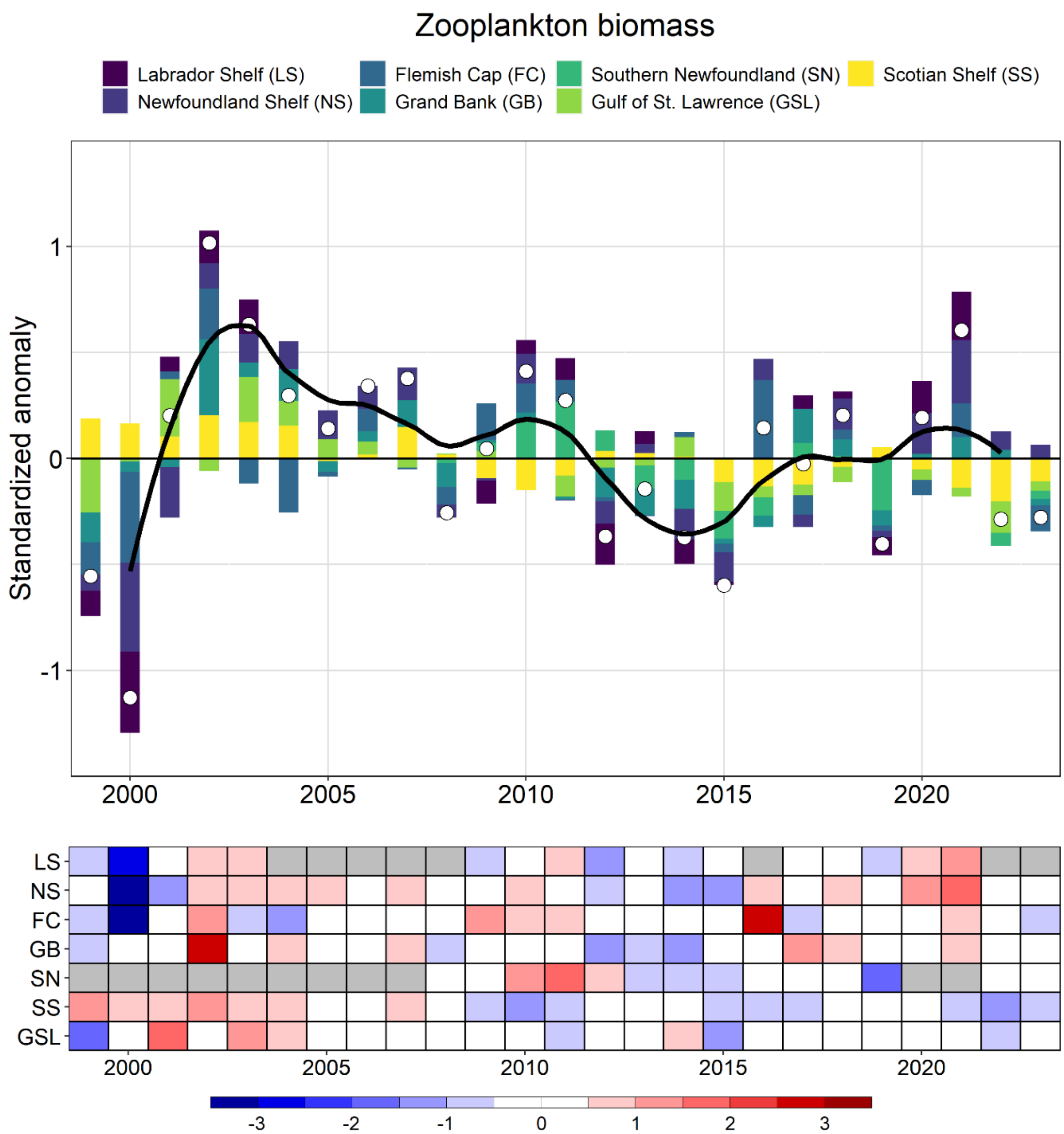

Figure 7. Top: Trends in mean annual anomalies of total zooplankton biomass. White open circle indicate mean annual anomalies for the Canadian Northwest Atlantic zone. Color bars indicate the relative contribution of each regions to the mean anomaly. The black line is a 3-year moving average showing the main temporal trends across the zone. Bottom: Scorecards of annual anomalies of zooplankton biomass. White cells indicate near-normal conditions, i.e., within ± 0.5 standard deviation from the climatological mean. Blue (red) cells indicate conditions below (above) the climatological mean. Regions are listed from north to south on the left. Anomalies were calculated based on a 1999-2020 climatological period.

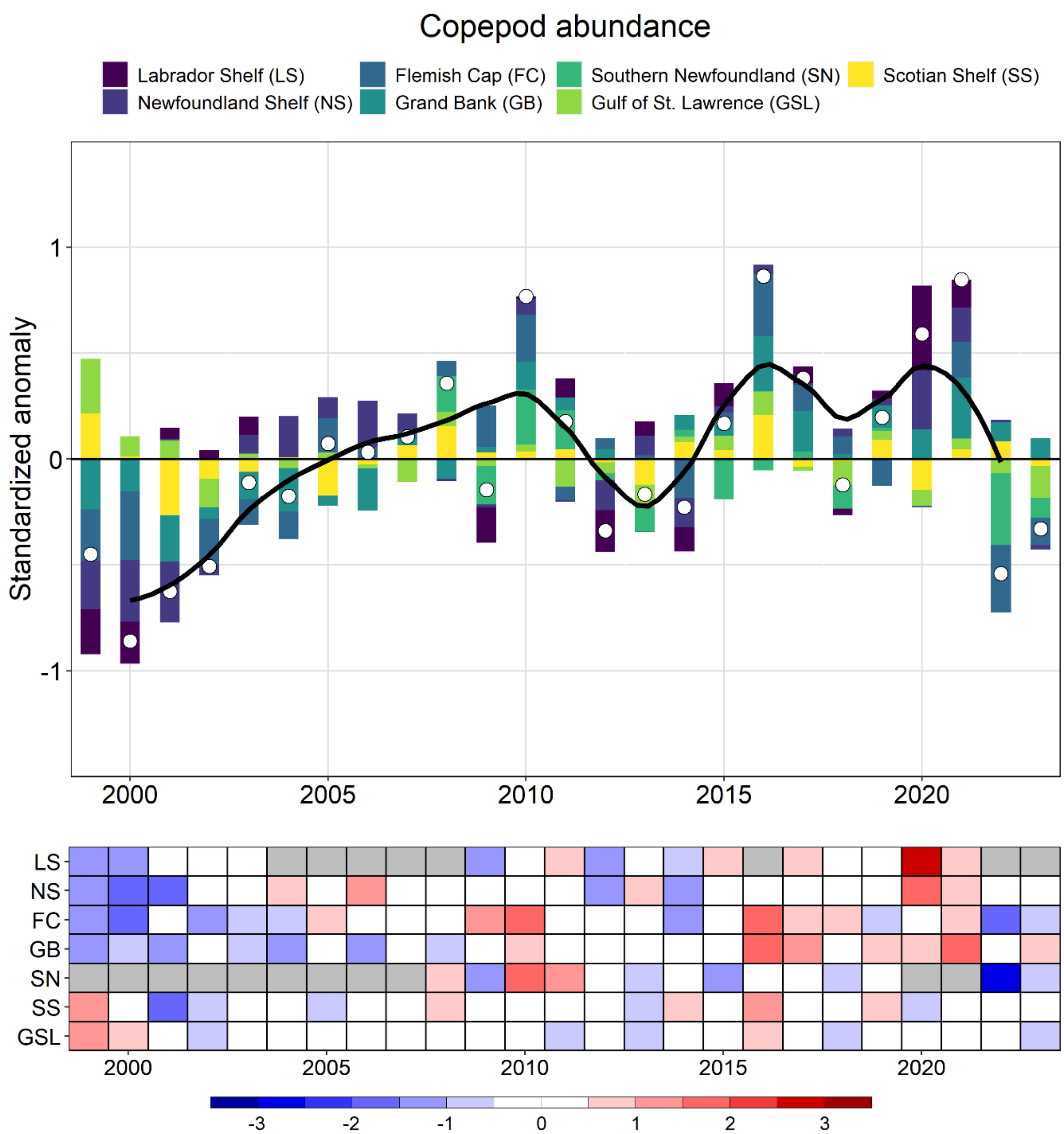

Figure 8. Top: Trends in mean annual anomalies of total copepod abundance. White open circle indicate mean annual anomalies for the Canadian Northwest Atlantic zone. Color bars indicate the relative contribution of each regions to the mean anomaly. The black line is a 3-year moving average showing the main temporal trends across the zone. Bottom: Scorecards of annual anomalies of copepod abundance. White cells indicate near-normal conditions, i.e., within ± 0.5 standard deviation from the climatological mean. Blue (red) cells indicate conditions below (above) the climatological mean. Regions are listed from north to south on the left. Anomalies were calculated based on a 1999-2020 climatological period.

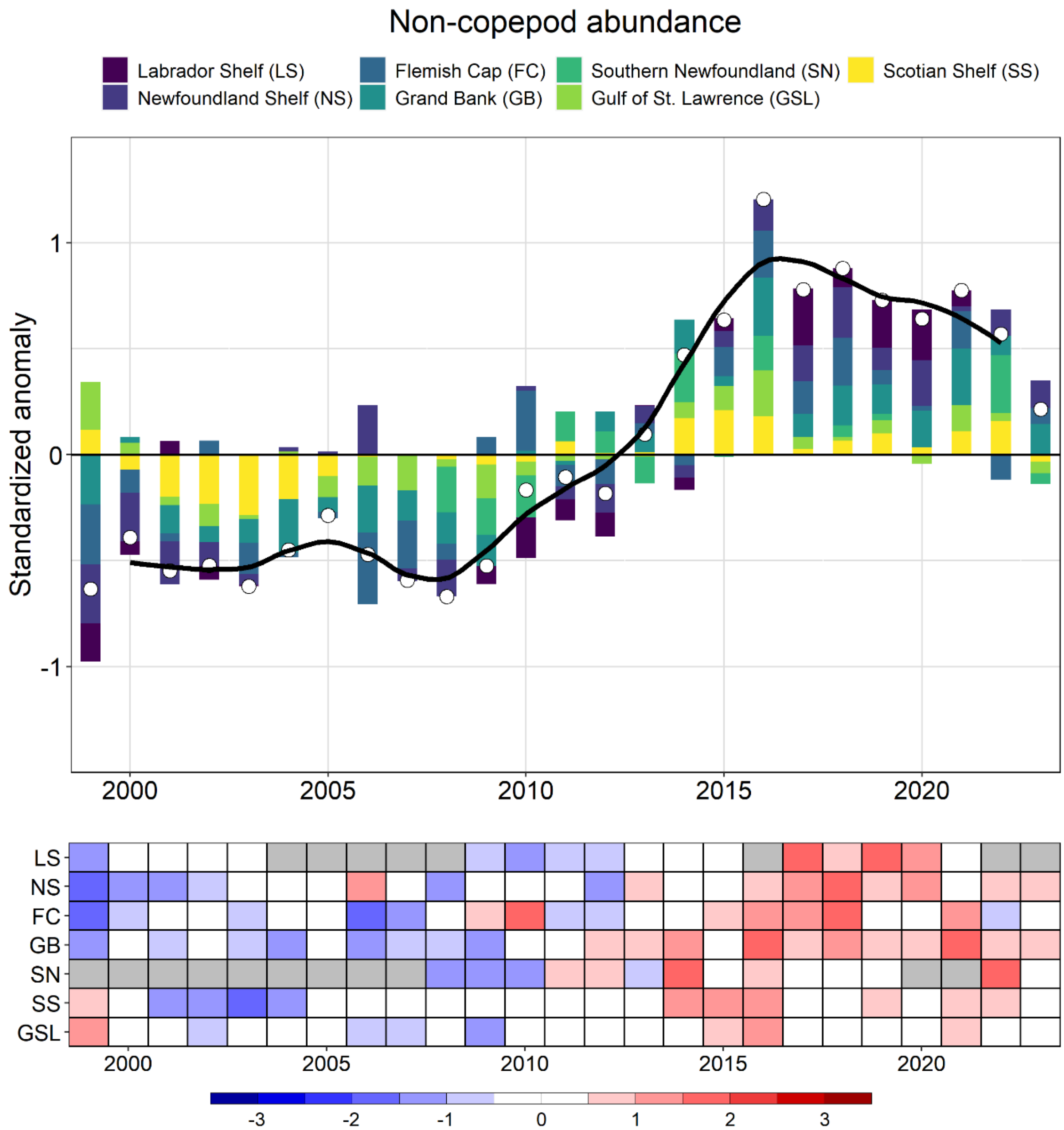

Figure 9. Top: Trends in mean annual anomalies of non-copepod abundance. White open circle indicate mean annual anomalies for the Canadian Northwest Atlantic zone. Color bars indicate the relative contribution of each regions to the mean anomaly. The black line is a 3-year moving average showing the main temporal trends across the zone. Bottom: Scorecards of annual anomalies of non-copepod abundance. White cells indicate near-normal conditions, i.e., within ± 0.5 standard deviation from the climatological mean. Blue (red) cells indicate conditions below (above) the climatological mean. Regions are listed from north to south on the left. Anomalies were calculated based on a 1999-2020 climatological period.

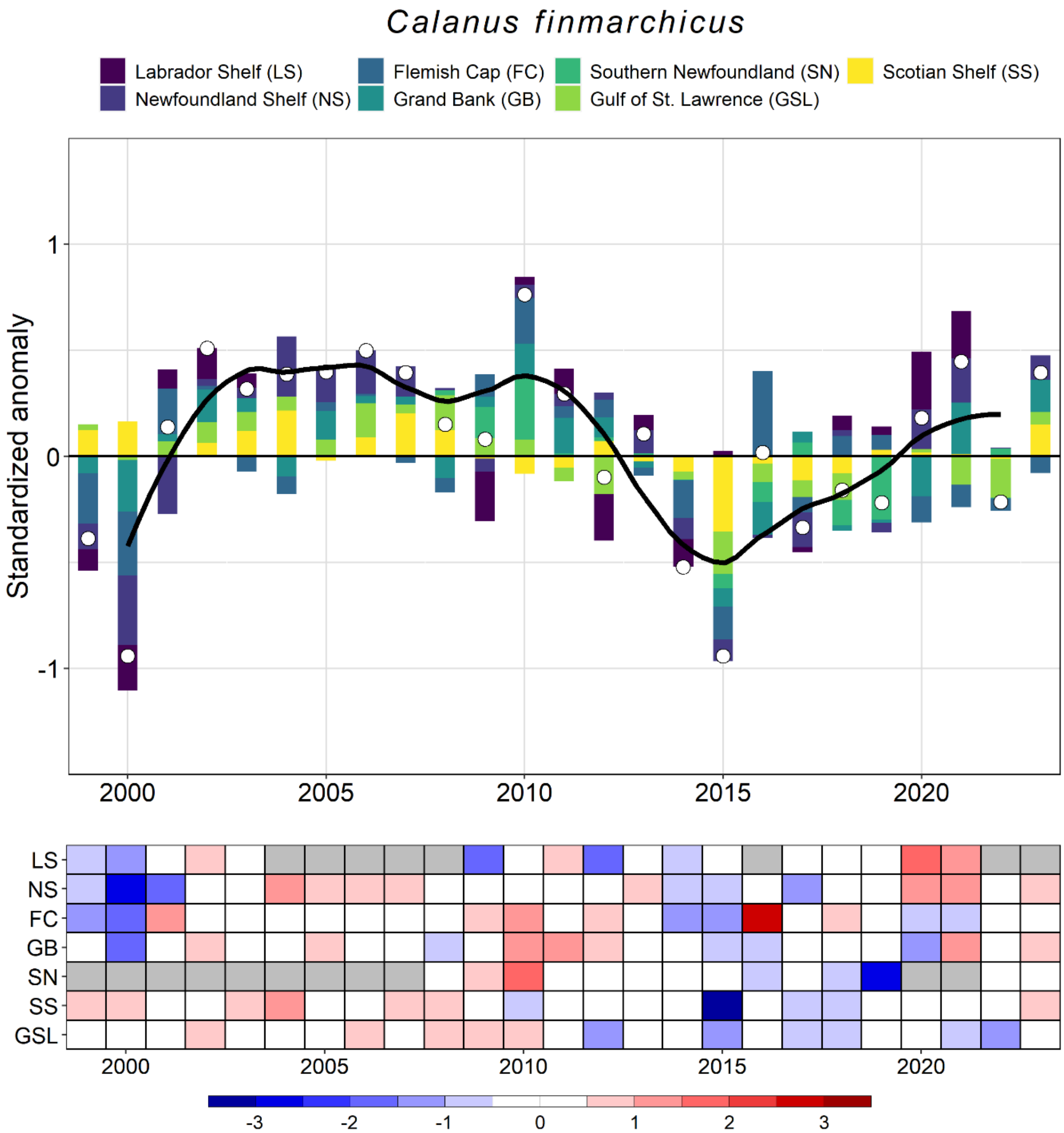

Figure 10. Top: Trends in mean annual anomalies of *Calanus finmarchicus* abundance. White open circle indicate mean annual anomalies for the Canadian Northwest Atlantic zone. Color bars indicate the relative contribution of each regions to the mean anomaly. The black line is a 3-year moving average showing the main temporal trends across the zone. Bottom: Scorecards of annual anomalies of *Calanus finmarchicus* abundance. White cells indicate near-normal conditions, i.e., within ± 0.5 standard deviation from the climatological mean. Blue (red) cells indicate conditions below (above) the climatological mean. Regions are listed from north to south on the left. Anomalies were calculated based on a 1999-2020 climatological period.

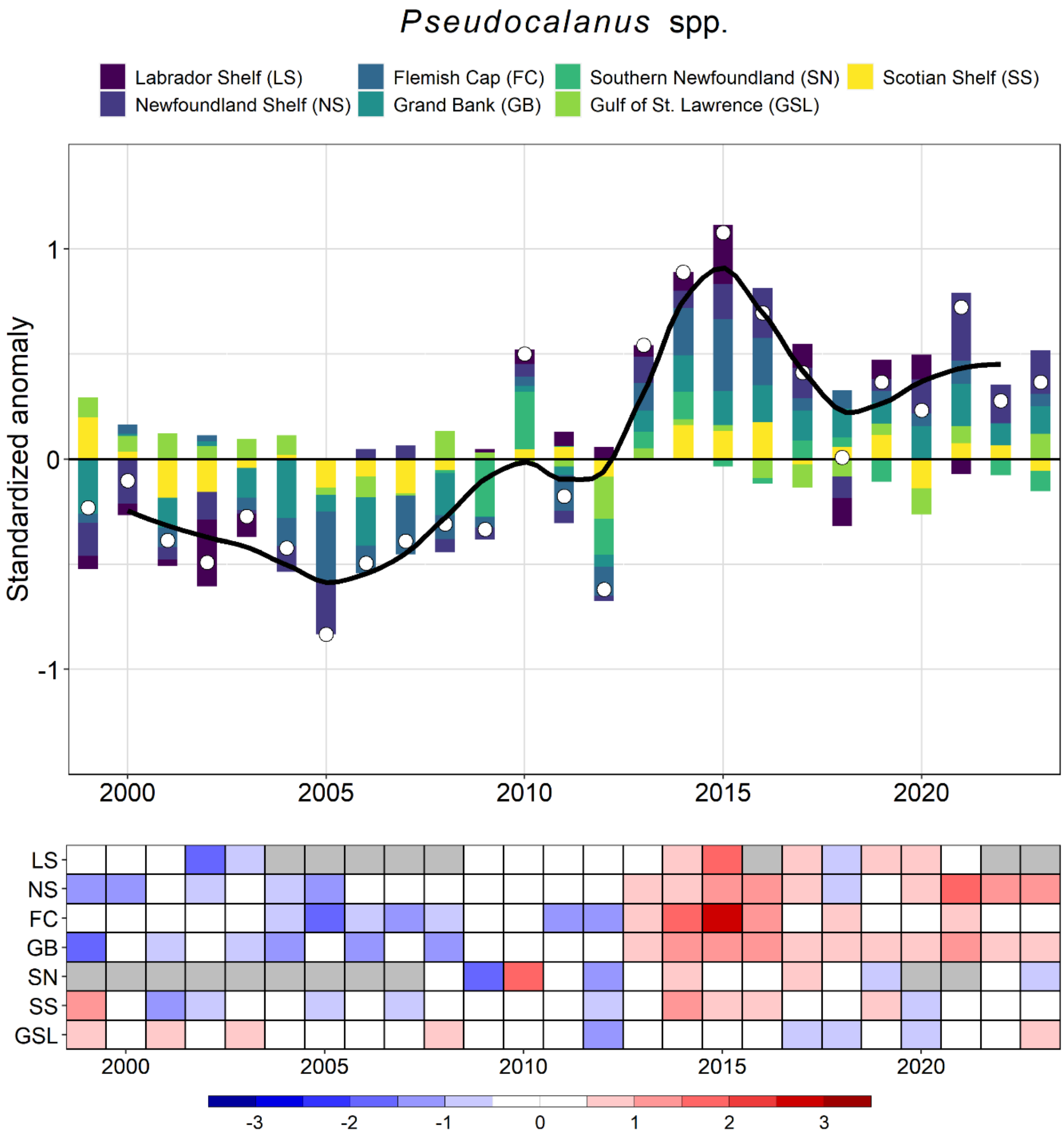

Figure 11. Top: Trends in mean annual anomalies of *Pseudocalanus* spp. abundance. White open circle indicate mean annual anomalies for the Canadian Northwest Atlantic zone. Color bars indicate the relative contribution of each regions to the mean anomaly. The black line is a 3-year moving average showing the main temporal trends across the zone. Bottom: Scorecards of annual anomalies of *Pseudocalanus* spp. abundance. White cells indicate near-normal conditions, i.e., within ± 0.5 standard deviation from the climatological mean. Blue (red) cells indicate conditions below (above) the climatological mean. Regions are listed from north to south on the left. Anomalies were calculated based on a 1999-2020 climatological period.

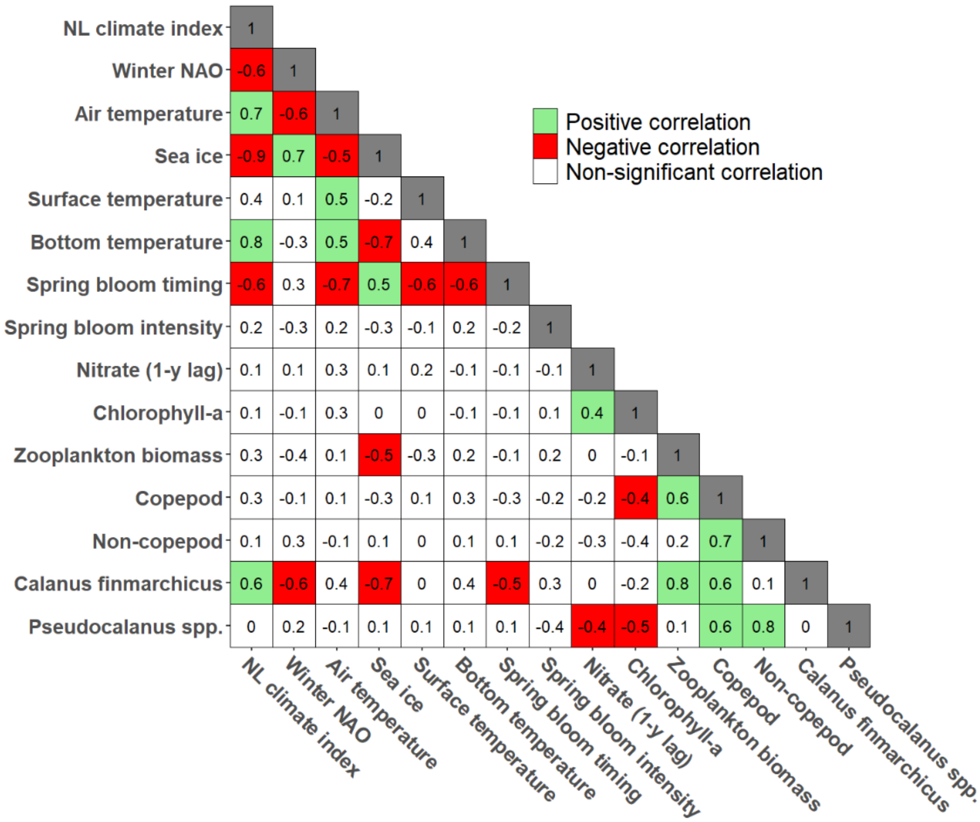

Figure 12. Correlation matrix summarizing the relationships between physical (Newfoundland and Labrador climate index, winter North Atlantic Oscillation [NAO] index, air temperature, sea ice cover, sea surface temperature, and bottom temperature), and biogeochemical (phytoplankton spring bloom peak timing and intensity; integrated deep nitrate [50-150 m]; integrated chlorophyll *a* [0-100 m]; total zooplankton biomass; abundance of copepod, non-copepod, *Calanus finmarchicus*, *Pseudocalanus* spp.) indices for the Southern Newfoundland, Grand Bank, Flemish Cap, Newfoundland Shelf, and Labrador Shelf EPUs from 1999 to 2023. Green cells indicate significant positive correlation, red cells indicate significant negative correlation, and white cells indicate non-significant correlations. Numbers in cells are Pearson correlation coefficients (*r*). Significance level for Pearson correlation tests was α=0.05.